

‘Green’ composites from soy based plastic and pineapple leaf fiber: fabrication and properties evaluation

Wanjun Liu^a, Manjusri Misra^a, Per Askeland^a, Lawrence T. Drzal^a, Amar K. Mohanty^{b,*}

^aComposite Materials and Structures Center, 2100 Engineering Building, Michigan State University, East Lansing, MI 48824, USA

^bThe School of Packaging, 130 Packaging Building, Michigan State University, East Lansing, MI 48824, USA

Received 10 September 2004; received in revised form 20 December 2004; accepted 6 January 2005

Abstract

Soy based bioplastic and pineapple leaf fiber ‘Green’ composites were manufactured using twin-screw extrusion and injection molding. Thermal properties, mechanical properties and morphology of the green composites were evaluated with Dynamic Mechanical Analyzer (DMA), United Testing System (UTS) and Environmental Scanning Electron Microscopy (ESEM). The effects of fiber loading and polyester amide grafted glycidyl methacrylate (PEA-g-GMA) as compatibilizer on morphology and physical properties of pineapple leaf fiber reinforced soy based biocomposites were investigated. The mechanical properties including tensile properties, flexural properties and impact strength of the biocomposites increased with increasing fiber content and the presence of the compatibilizer. ESEM studies reveal that the dispersion of fiber in the matrix became worse with increasing fiber content but improved with addition of compatibilizer. The addition of the compatibilizer also decreased the water absorption. The improved mechanical properties of the composites correspond, in the presence of the compatibilizer, is attributed to interactions between hydroxyl groups in the pineapple leaf and epoxy groups in PEA-g-GMA.

© 2005 Elsevier Ltd. All rights reserved.

Keywords: Green composites; Soy based bioplastic; Pineapple leaf fiber

1. Introduction

The ever-growing environmental pressure caused by the widespread consumption of petroleum based polymers and plastics have spurred a thrust into the development of biodegradable or environmentally acceptable materials. Biopolymers derived from various natural botanical resources such as protein and starch have been regarded as alternative materials to petroleum plastic because they are abundant, renewable, inexpensive and biodegradable. Domestic cultivation of soybeans has led a great deal of research into the development of biopolymers derived from their byproducts, such as soy protein. Soy proteins are complex macromolecules containing 20 amino acids [1] with many sites available for interaction with a plasticizer. Therefore, soy protein can be converted to soy protein plastic through extrusion with a plasticizer or cross-linking

agent [2–4]. Although the mechanical properties of soy protein plastic can be controlled and optimized by adjusting the molding temperature and pressure or processing parameter and initial moisture content [5–7], the application of soy protein plastic is limited because of its low strength and high moisture absorption. The most effective method is to blend soy protein plastic with biodegradable polymer to form soy protein based biodegradable plastic. Currently, the biodegradable plastics being used to blend soy plastic include polyester amide, polycaprolactone, Biomax[®], poly(tetramethylene adipate-co-terephthalate) [8–10], whose processing window matches with that of soy protein plastic.

Fiber reinforced composites will increase the use of these materials and their application into various arenas such as automotive and packaging products. Natural fibers such as kenaf, flax, jute, hemp, sisal, and henequen fiber reinforced composites are an attractive research area because natural fibers are eco-friendly, sustainable, low cost, low density, with acceptable mechanical properties, ease of separation,

* Corresponding author. Tel.: +1 517 355 3603; fax: +1 517 353 8999.
E-mail address: mohantya@msu.edu (A.K. Mohanty).

carbon dioxide sequestration and biodegradability [11,12]. Additionally, these fibers have excellent thermal and sonic insulation properties. Natural fibers from grass, hemp, and ramie have already been reported as reinforcements for soy based matrices [13–15]. Improvements of the physical properties of these composites via surface treatments and fiber loading have been examined [13,14]. Although both soy plastics and natural fibers have polar groups such as hydroxyl and carboxyl groups that can have some physical interactions during processing, these physical interactions are limited and typically do not lead to significant improvements in performance. The concentration of matrix–fiber interaction can be boosted with compatibilizer interact with both fiber and polymer. However, little work has focused on the incorporation of compatibilizer into natural fiber reinforced soy based biocomposites, which will be discussed in this paper. Pineapple leaf fiber (PALF) was selected as reinforcement materials for soy based biocomposites system due to the following reasons. First, PALF has good tensile strength (400–1600 MPa) and modulus (59 GPa) due to its high cellulose content 70–82% and high degree of crystallinity [12,16]. Second, since pineapple can be cultivated throughout the southern USA, it is possible for significant domestic production of PALF. Third, PALF has already been used as a reinforcement to strengthen LDPE, rubber, thermosetting polyester, polyhydroxybutyrate (PHB) and polyester amide [17–21], but never used to reinforce soy based bioplastic.

In this work, new bioplastic/natural fiber composites were fabricated and tested. Soy protein plastic was blended with polyester amide, a random copolymer of aliphatic polyester and Nylon-6, to form soy based bioplastics. Polyester amide was chosen for the potential compatibility between its amide groups and the soy protein plastic. PALF was used to reinforce the soy-based bioplastic to form composite materials. The use of these composites will reduce the dependence on petroleum products, save energy, bring benefit to environment and reduce environmental pollution from petroleum product. The influence of fiber loading and using PEA-g-GMA as compatibilizer on physical properties of PALF reinforced soy based biocomposites was studied with morphology/structure characterization and mechanical properties measurements.

2. Experimental

2.1. Materials

Soy flour (Defatted Soy flour number 063-130) with 52% protein was obtained from Archer Daniels Midland Company (Decatur, IL). Glycerol is used as the plasticizer for soy flour and was obtained from J.T. Baker (Phillipsburg, NJ). The polyester amide (BAK 1095) was obtained from Bayer Corp. (Pittsburgh, PA). Pineapple leaf fiber was purchased from India. Polyester amide grafted glycidyl

methacrylate (PEA-g-MA) was used as compatibilizer in this system, which is already described by the authors in a previous study [22].

2.2. Samples preparation

2.2.1. Extrusion

Soy flour, polyester amide and the chopped PALF (6 mm length) were all dried in a vacuum oven at 80 °C. Soy flour was pre-mixed with the plasticizer in a weight ratio of 70:30 with a kitchen mixer for 30 min. This mixture was fed into a twin-screw extruder ZSK 30 (Werner-Pfleiderer) ($L/D=30$) which has six individually controllable zones. The zone temperatures for blending soy flour and glycerol were maintained at 95, 105, 115, 125, 130 and 130 °C, respectively. The extruder was operated at 100 rpm. This plasticized soy flour was collected in the form of strands which were then pelletized and mixed with the polyester amide in the weight ratio of 1:1.

This mixture was fed into the extruder with all the zone temperatures at 130 °C and a screw speed of 100 rpm. The resulting soy flour based polyester amide bio-plastic (soy based bioplastic) was collected and pelletized. The soy based bio-plastic was extruded with 15, 30-wt% PALF and 30 wt% PALF with addition of 5 wt% PEA-g-GMA as compatibilizer with processing temperature of 130 °C and screw speed of 100 rpm. The samples were pelletized.

2.2.2. Injection molding

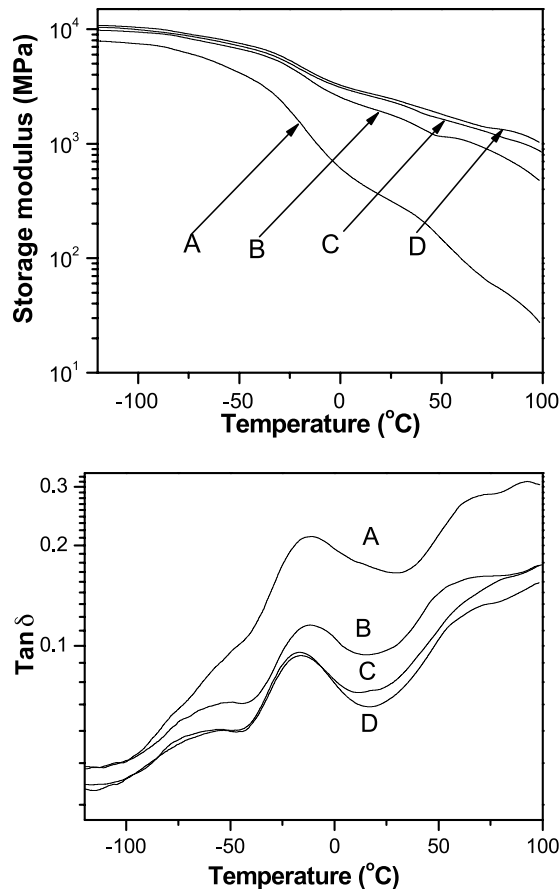
The bioplastic and PALF reinforced biocomposites were injection molded in an 85-ton Cincinnati-Milacron injection molder with processing temperature of 130 °C. Injection molded standard specimens were obtained for mechanical and thermal testing.

2.2.3. Mechanical properties measurements

The tensile properties and flexural properties of injection molded specimens were measured with a United Testing System SFM-20 according to ASTM D638 and ASTM D790, respectively. System control and data analysis was performed using the Datum software package. The notch impact strength was measured with a Testing Machines Inc. 43-02-01 Monitor/Impact machine according to ASTM D256. In all mechanical properties measurement, five specimens were measured for each sample.

2.2.4. Dynamic mechanical properties of biocomposites

A dynamic mechanical analyzer (2980 DMA, TA instruments, USA) was used to measure dynamic mechanical properties of the biocomposites. DMA multi-frequency and 3 point bending mode were used with frequency of 1 Hz. Span length of 3 point bending was 50 mm. The initial force was 0.05 N. The heating rate was 4 °C/min. Tests were performed from –100 to 100 °C.



A= soy based bioplastic

B= 15wt% PALF reinforced soy composites

C= 30wt% PALF reinforced biocomposites

D= 30wt% PALF with 5% PEA-g-GMA reinforced biocomposites

Fig. 1. Dynamic mechanical properties of PALF reinforced soy based biocomposites.

2.2.5. Heat deflection temperature (HDT) measurement

The HDT behaviour of the biocomposites was measured with dynamic mechanical analyzer (2980 DMA, TA instruments, USA) at a load of 455 kPa according to ASTM D648 under DMA control force and 3 point bending mode with a heating rate of 2 °C/min.

2.2.6. Environmental scanning electron microscopy (ESEM) observation

The tensile fracture surfaces and surface fractured in liquid nitrogen were observed with Phillips Electroscan 2020 environmental scanning electron microscope (ESEM) with an accelerating voltage of 20 kV.

2.2.7. FTIR measurement

PALF fibers were pulverized and compressed in KBr to form pellets. Thin films of polyester amide and PEA-g-GMA, and mixture of PALF with PEA-g-GMA (from microextruder mixing) were made by thermal compression

molding with temperature of 140 °C. A Perkin Elmer system 2000 FTIR Spectrometer was used to analysis the structure of above samples.

2.2.8. Water absorption measurement

Water absorption of PALF reinforced soy based biocomposites and soy based bioplastic were measured according to ASTM D570-81. Soy based bioplastic and biocomposites were dried in an oven at 50 °C for 24 h and cooled in a desiccator before weighting. These samples were submerged in distilled water for a designated period of time. Water on the surface of the samples was removed and the samples' weight was measured. In order to check the water-soluble content of samples during soaking, samples were dried at 50 °C for 24 h and then the weight loss of the samples was determined. The sum of the weight gain following soaking plus the weight loss after drying is defined as the total absorbed water.

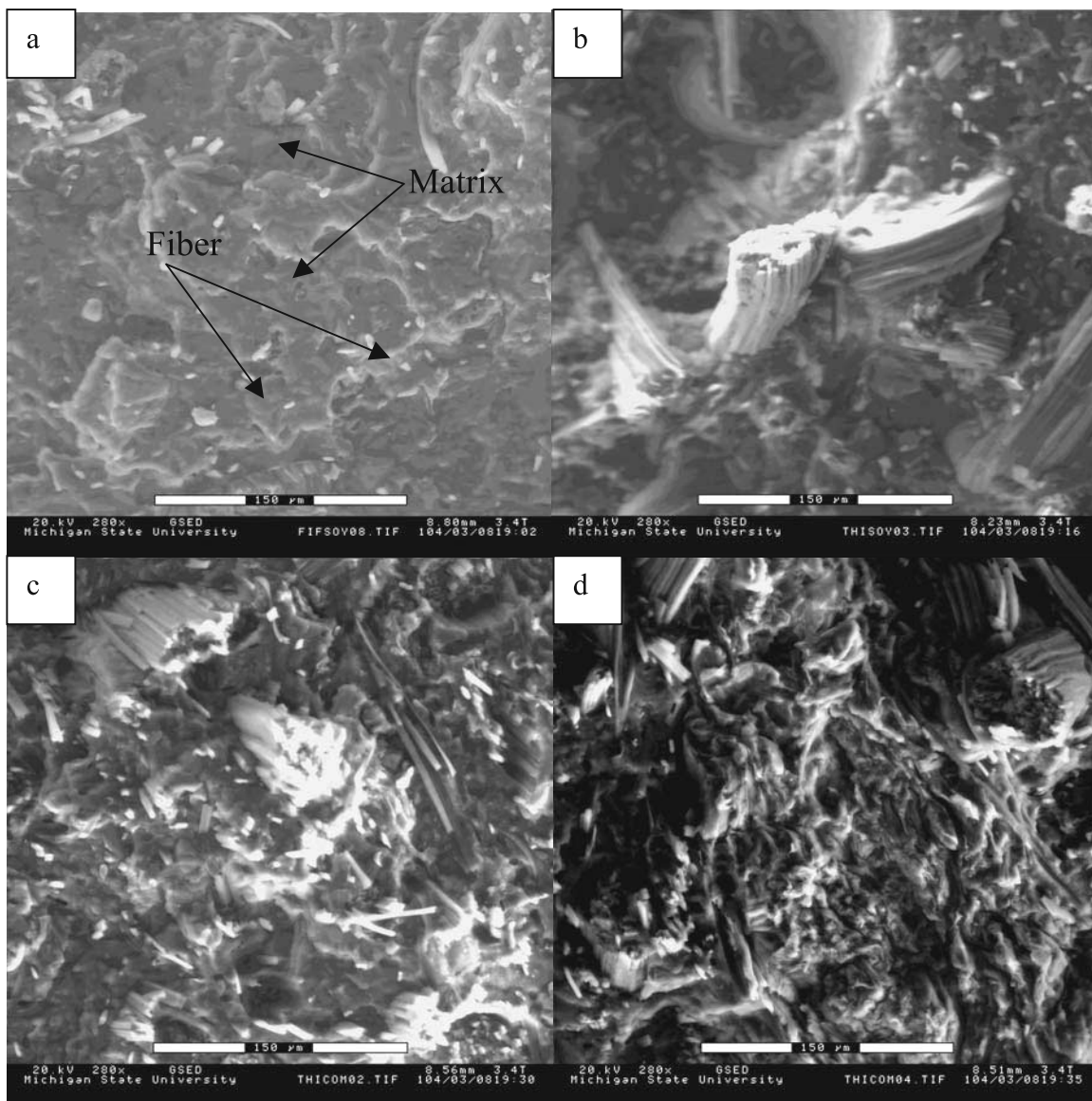


Fig. 2. ESEM micrographs (280 \times with scale bar of 150 μm) of (a) 15 wt% PALF soy composites; (b) 30 wt% PALF soy composites; (c) and (d) 30 wt% PALF with 5 wt% PEA-g-GMA soy composites (fractured in liquid nitrogen).

3. Results and discussion

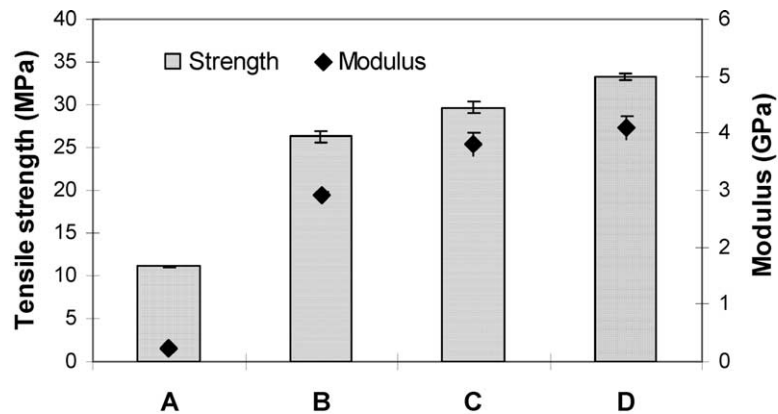
3.1. Dynamic mechanical properties of composites

The storage modulus of the soy based bioplastics, as obtained from the DMA tests (Fig. 1), increases upon addition of PALF and continues to increase with increasing PALF loading. In addition, the storage modulus of the 30 wt% PALF fiber reinforced composites increased after adding 5 wt% of the compatibilizer. The compatibilizer may improve the dispersion of the fiber resulting in an increase in fiber reinforcement efficiency. It was also found that the peak value of $\tan \delta$ in the glass transition region decreased upon addition of PALF fiber. It is well known that the damping in the transition zone measures the imperfection in the elasticity and that much of the energy used to deform a

material during DMA testing is dissipated directly into heat [23]. This indicates that after adding PALF fiber, the molecular mobility of the composites decreased and the mechanical loss to overcome inter-friction between molecular chains is reduced. Generally, the damping of the polymer is much greater than that of the fibers. Thus, addition of fibers to polymeric materials will increase the elasticity and decrease the viscosity and hence less energy will be used to overcome the frictional forces between molecular chains as to decrease mechanical loss.

3.2. Dispersion of fiber in matrix

Micrographs taken at 200 \times easily describe the PALF fiber dispersion in the matrix (Fig. 2). Typically, two types of regions were found for the composites: regions indicative



A= soy based bioplastic

B= 15wt% PALF reinforced soy composites

C= 30wt% PALF reinforced biocomposites

D= 30wt% PALF with 5% PEA-g-GMA reinforced biocomposites

Fig. 3. Tensile properties of PALF reinforced soy based biocomposites.

of good dispersion with small fiber size (suggesting good separation) and regions indicative of poor dispersion with aggregate fibers with larger size. At the 15 wt% loading, it was observed that most of the PALF fibers separated and only a small amount of the fibers were aggregated. However, aggregation with a larger fiber size was common in the 30 wt% PALF reinforced composites. This indicates that the fiber dispersion worsens with increasing fiber loading. At higher loadings the probability of interfiber contact increases and thus the extent of fiber aggregation will surely follow. When the compatibilizer was added to the 30 wt% fiber reinforced composites the fibers became more disperse in the matrix as noted by the decreased area of the fiber aggregates and increased separation of fibrous regions. One possible explanation is that the compatibilizer

diffuses to the interface between fiber and matrix so as to interact with the fibers. Therefore, during processing under interaction forces between the fiber and compatibilizer, the cementing force in interfiber region is overcome and hence the fiber is more easily dispersed into the matrix. A benefit of the increased dispersion, of course, is an increase in the contact area between fiber and matrix and an increase in the aspect ratio of the fiber, improving its effectiveness as reinforcement.

3.3. Mechanical properties

The tensile properties of the composites are shown in Fig. 3. It was found that the tensile strength and modulus of composites increased with PALF content. The tensile modulus and strength of the 30 wt% fiber loading increased by 2 and 18 times compared to those of soy-based bioplastics, respectively. It was also found that the tensile strength and modulus improved with addition of compatibilizer to the 30 wt% PALF fiber reinforced biocomposites, indicating that the PEA-g-GMA is an effective compatibilizer for this system and successfully transferred the stress from matrix to fiber. The stress–strain curves of the composites are in Fig. 4. Soy based bioplastic had elongation of 53%, but 15 and 30% PALF reinforced had elongation of 2.29 and 1.81%. This showed that elongation of the composites reduced with increasing fiber content. The addition of the compatibilizer did not affect the elongation, though the stress increased. The flexural properties of the composites are shown in Fig. 5. The flexural strength and modulus improved by 3 and 15 times, respectively with 30-wt% fiber loading. In addition, the presence of the

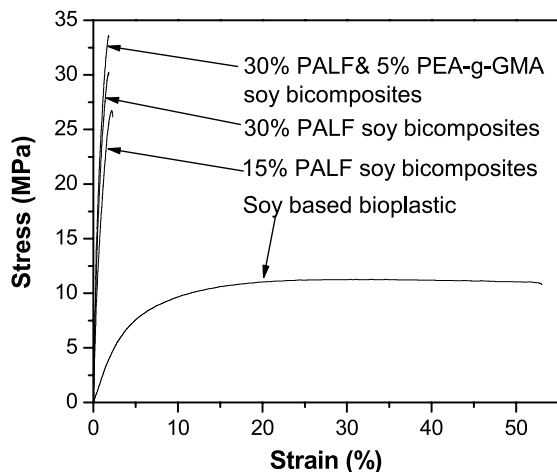
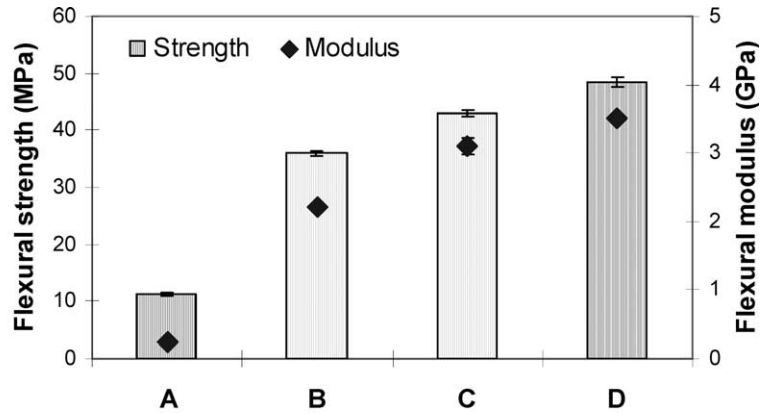


Fig. 4. Stress–strain curves of PALF reinforced soy based biocomposites.



- A= soy based bioplastic**
- B= 15wt% PALF reinforced soy composites**
- C= 30wt% PALF reinforced biocomposites**
- D= 30wt% PALF with 5% PEA-g-GMA reinforced biocomposites**

Fig. 5. Flexural properties of PALF reinforced soy based biocomposites.

compatibilizer also increased the flexural strength and modulus of the composites. This indicates that the flexural and tensile properties followed the same trend.

The rule of mixtures was used to predict the modulus of fiber-reinforced composites. Since many of the equations proposed by various authors are either complex or unpractical, a simple equation modified from aligned continuous fiber reinforced composites [24] was used to predict the tensile modulus and tensile strength results of natural fiber reinforced soy based green composites. The predicted moduli of the composites were determined from Eq. (1).

$$E_c = \xi_E V_f E_f + V_m E_m \quad (1)$$

Where E_c , is the modulus of the composite, ξ_E is the fiber efficiency factor of the composite modulus considering the effects of fiber length and orientation, E_f is the modulus of fiber, V_f is the volume fraction of fiber, E_m is the modulus of matrix, V_m is the volume fraction of matrix.

The predicted strengths of the composites were determined from Eq. (2).

$$\sigma_c = \xi_\sigma V_f \sigma_f + V_m \sigma_m \quad (2)$$

Where σ_c , is the strength of the composites, ξ_σ is the fiber efficiency factor for composite strength considering the effects of fiber length and orientation, σ_f is the strength of fibers, V_f is the volume fraction of fiber, σ_m is the strength of matrix, V_m is the volume fraction of matrix.

The weight fractions of PALF were converted to volume fraction by using the following equation.

$$V_i = \frac{W_i/\rho_i}{\sum W_i/\rho_i} \quad (3)$$

Where V_i , W_i , and ρ_i are the volume fraction, weight fraction and density of the component i in the composites, respectively. Densities of 1.44 g/cm³ and 1.21 g/cm³ were taken for PALF and soy based bioplastic, respectively.

The tensile modulus and strength of PALF reinforced composites vs. fiber volume fraction trend is shown in Fig. 6. It was found that tensile modulus and strength increased with increasing fiber volume fraction but not linearly. In contrast, the slope decreased with increasing fiber volume fraction. In this case, curve fitting of modulus and strength vs. fiber volume fraction does not have any meaning. Therefore, Eqs. (1) and (2) were used to calculate the fiber efficiency factor for modulus and strength of the

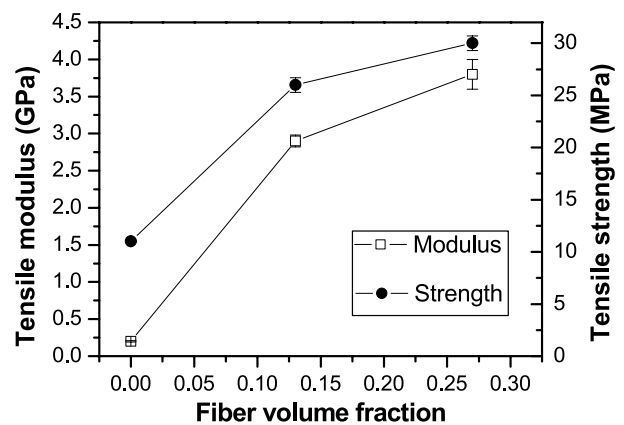
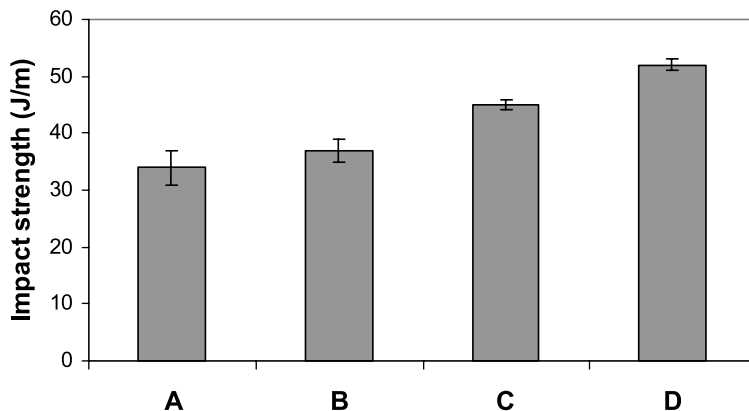


Fig. 6. Plots of tensile strength and modulus vs. fiber volume fraction of PALF reinforced soy based biocomposites.



A= soy based bioplastic

B= 15wt% PALF reinforced soy composites

C= 30wt% PALF reinforced biocomposites

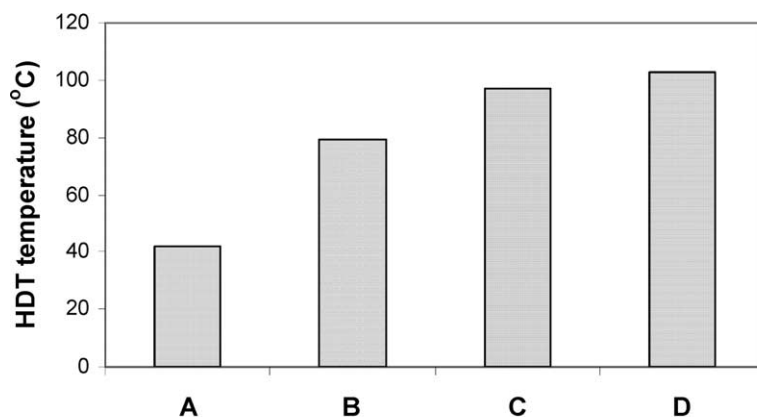
D= 30wt% PALF with 5% PEA-g-GMA reinforced biocomposites

Fig. 7. Impact strength of PALF reinforced soy based biocomposites.

Table 1

Fiber efficiency factor of PALF reinforced soy based composites

Fiber reinforcement efficiency factor for strength and modulus	15 wt% PALF fiber reinforced soy composites	30 wt% PALF fiber reinforced soy composites	30 wt% PALF fiber with 5 wt% PEA-g-GMA reinforced soy composites
Fiber efficiency factor for modulus	0.36 ± 0.01	0.23 ± 0.01	0.25 ± 0.01
Fiber efficiency factor for strength	0.13 ± 0.005	0.08 ± 0.002	0.09 ± 0.001



A= soy based bioplastic

B= 15wt% PALF reinforced soy composites

C= 30wt% PALF reinforced biocomposites

D= 30wt% PALF with 5% PEA-g-GMA reinforced bio composites

Fig. 8. Heat deflection temperature of PALF reinforced soy based biocomposites.

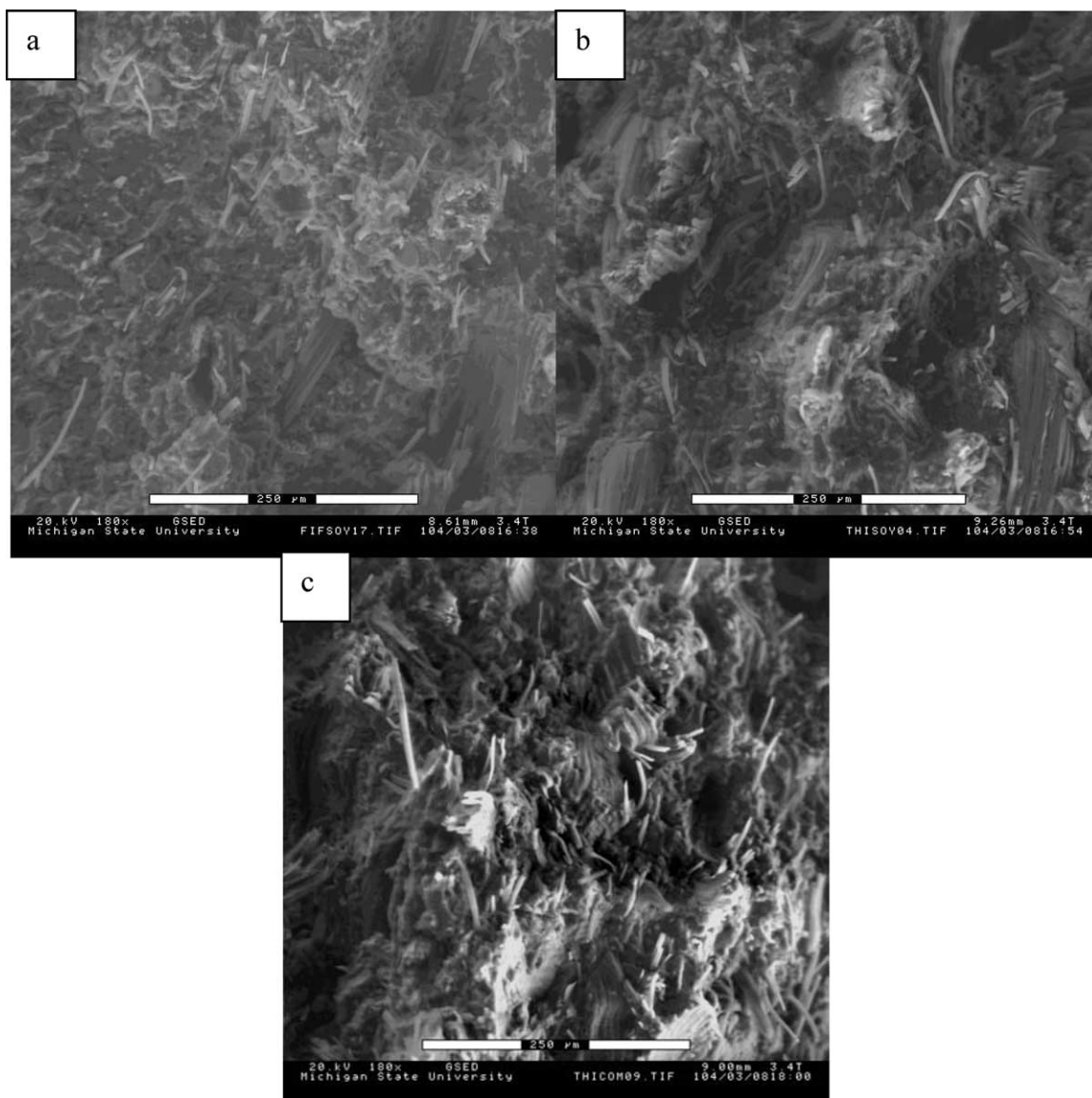


Fig. 9. ESEM micrographs of (a) (180 \times) with scale bar of 250 μ m, 15 wt% PALF soy composites; (b) (180 \times) with scale bar of 250 μ m, 30 wt% PALF soy composites; (c) (180 \times) with scale bar of 400 μ m, 30 wt% PALF with 5 wt% PEA-g-GMA soy composites (tensile fracture surface).

composites with different compositions. Results are shown in Table 1. It was found that the fiber efficiency factor of the modulus decreased with increasing fiber contents and increased after addition of the compatibilizer. The value is lower than expected but reasonable for natural fiber reinforced composites [25]. Similarly, the fiber efficiency factor for strength decreased with increasing fiber contents, but increased with addition of compatibilizer. A decrease in the fiber orientation along the flow direction of the matrix, due to fiber aggregation, led to the decrease in the fiber reinforcement efficiency factor. This explains the relatively small increase in tensile strength after increasing the fiber volume fraction from 0.13 to 0.27.

The presence of PALF in the soy based bioplastics matrix led to improved impact strength (Fig. 7), most notably a 30% increase in the impact strength with the 30 wt% fiber

loaded specimen. This increase is the result of two factors. First, the fiber reduces the impact strength of the composite by drastically decreasing the break elongation. Hence, the area under the stress–strain curves is reduced because a new stress concentration will be formed around fiber ends. Second, the fibers reduce the crack propagation rate by forcing a crack around the fiber and bridging crack through fiber pullout [26,27] leading to an increase in the impact strength. In the present composite system, it is obvious that the hindrance effect of PALF on the crack propagation rate is greater than crack initiation of the fiber through forming new stress concentrations in the composites. Therefore, pineapple leaf has a positive contribution on its reinforced soy based ‘green’ composites.

Additionally, it was found that after adding the compatibilizer to the 30 wt% PALF composite, the impact

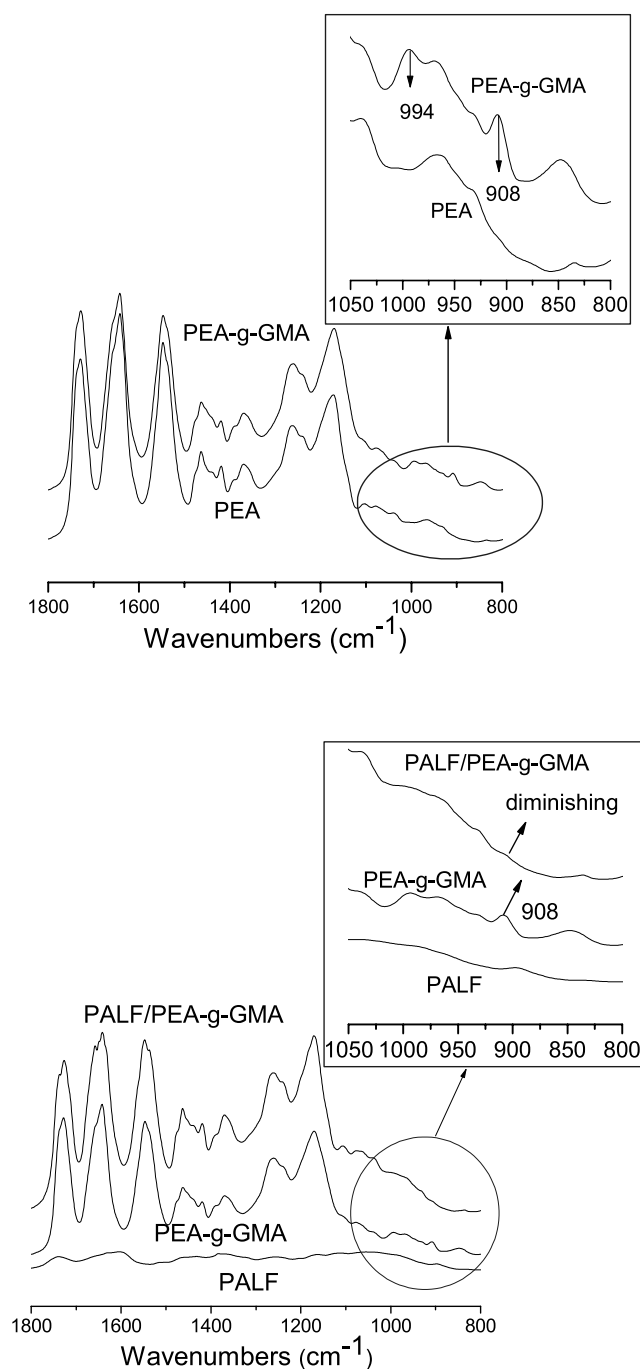


Fig. 10. FTIR spectra of PEA, PEA-g-GMA, PALF and their blends.

strength improved 20% compared with the composite without the compatibilizer. When compared with the soy based bioplastic, the impact strength improved by 50%. This result suggests that PEA-g-GMA played the role of an interfacial agent, which increases the adhesion between fiber and matrix.

3.4. Heat deflection temperature

The heat deflection temperature (HDT) is defined as the

temperature at which a material deflects by 0.25 mm under the application of a load (455 kPa). Fig. 8 gives the values of heat deflection temperatures of the bio-plastics and the bio-composites. The heat deflection temperature showed a significant increase of about 55 °C with a 30 wt% fiber loading. This is due to the significant improvement in modulus of 30 wt% PALF reinforced composites as compared with soy-based bioplastic. In addition, the HDT temperature of the composites increased with addition of PEA-g-GMA because of the increases in modulus.

3.5. Morphology of tensile fracture surface

Examinations of the morphology of the fracture surfaces show phase information and fracture characteristics, reflecting on why the mechanical properties have been changed and in turn deciding the mechanical properties of polymeric composites. The morphology of the tensile fracture surface of PALF reinforced bio-composites is shown in Fig. 9. As previously mentioned there was good fiber dispersion for the 15 wt% fiber reinforced composites. Most of fiber worked as a single fiber similar to glass fiber. Poor dispersion is apparent for the 30 wt% fiber reinforced composite as the fibers were bunched together. Since poor dispersion often results in the formation of stress concentrations in a composite, it is not too surprising that the mechanical strength does increase at higher fiber loadings. However, the presence of a compatibilizer reduces the fiber size and improves the fiber's dispersion, reflecting its effectiveness as an interfacial agent. Thus, the addition of compatibilizer increased the interaction between fiber and matrix and improved the mechanical properties of the composites. This leads to the question as to how the fiber and compatibilizer interact.

3.6. Interaction between fiber and compatibilizer

By examining the FTIR spectra of the PEA, PEA-g-GMA, PALF, PALF/PEA, and PALF/PEA-g-GMA (Fig. 10) a picture of how the compatibilizer interacts with the fiber could begin to be developed. The characteristic absorption peaks at 908 and 994 cm^{-1} of the epoxy group in glycidyl methacrylate were found in PEA-g-GMA, but those two peaks were not found in spectrum of PEA indicating that glycidyl methacrylate was grafted to the main chain of polyester amide [22,28]. After blending with the PALF, the characteristic peak of epoxy ring at 908 cm^{-1} diminished, however, the peak at 994 cm^{-1} remained pointing to an interaction between PALF and the epoxy group in the compatibilizer PEA-g-GMA. As it is well known that there is a high concentration of potentially active hydroxyl groups on the fiber surface, the decrease in concentration of the epoxy ring peak is indicative of a reaction between the compatibilizer and PALF surface. The interaction between PALF and PEA-g-GMA is shown in Scheme 1.

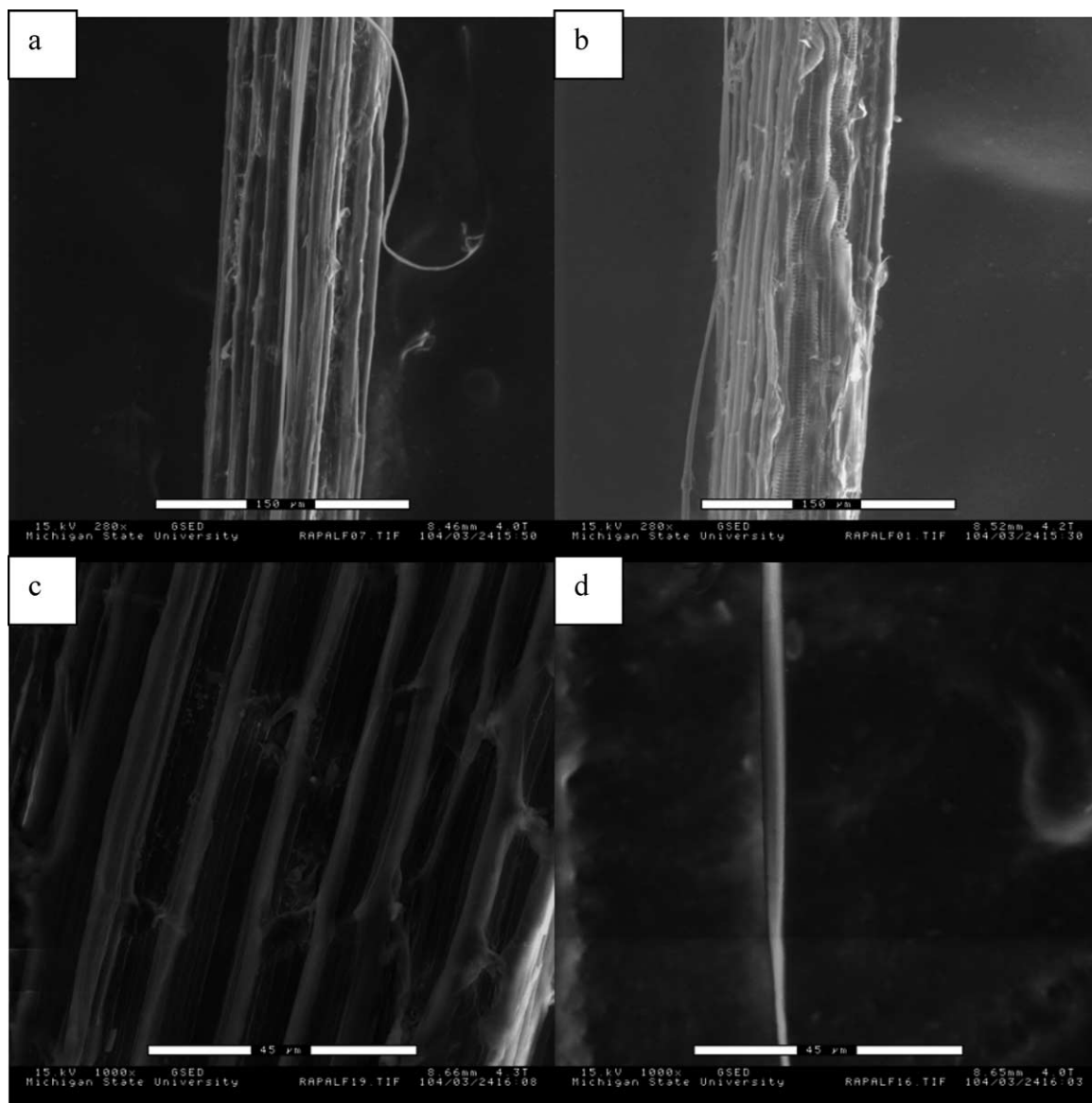
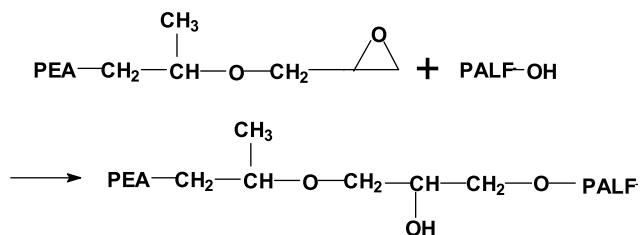


Fig. 11. ESEM micrographs of PALF (a) and (b) (280 \times) with scale bar of 150 μm ; (c) and (d) (1000 \times) with scale bar of 45 μm .

The interactions between the PALF and PEA-*g*-GMA will enhance the interfacial adhesion between fiber and matrix so that stresses are easily transferred from matrix to fiber and the mechanical properties including tensile, flexural and impact strength are improved. The changes in morphology, particularly the improvement in fiber



Scheme 1. Interaction between PALF fiber and PEA-*g*-GMA.

dispersion after its addition, display the effectiveness of PEA-*g*-GMA as a compatibilizer for this system.

3.7. Morphology change of fiber in composite

PALF consists of a fiber bundle with a diameter of approximately 100 μm (Figs. 11(a) and (b)) consisting of fibrils and material between the fibrils. This material consists of hemicellulose and lignin, which is typically found the surface of cellulose fibers to cement the individual fibrils. Careful observation of PALF found that the fibril diameter was around 4 μm (Fig. 11(c) and (d)).

After manufacture of the biocomposite, the morphology of the PALF changed (Fig. 12) as the individual fibrils were present in the 15 wt% composites and not the bundled fibers. The fiber diameter in the biocomposites was around 5 μm .

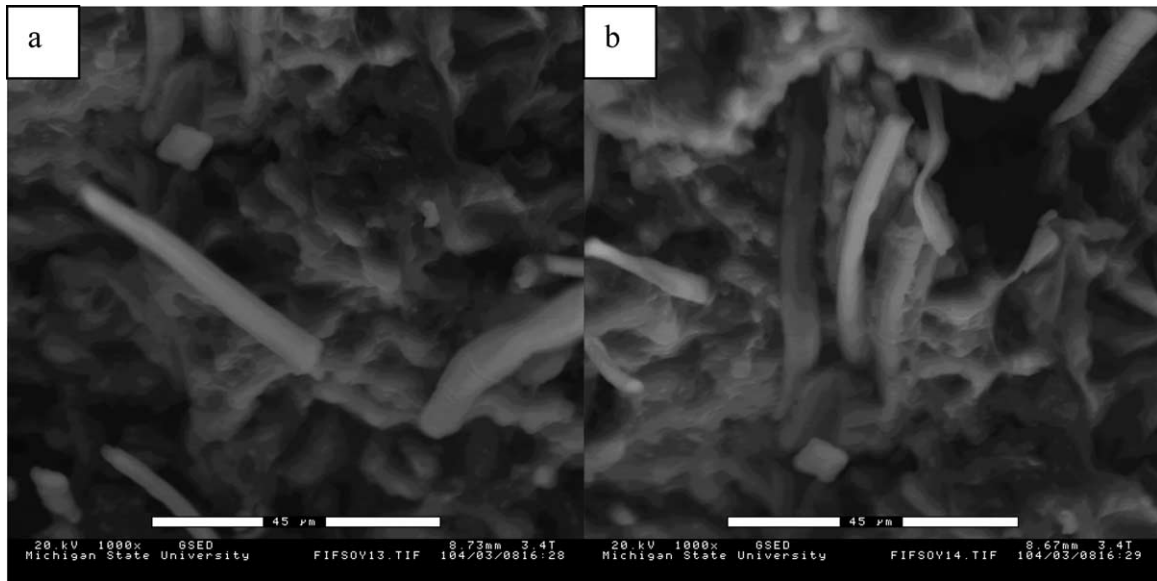


Fig. 12. ESEM micrographs of PALF in 15 wt% PALF soy based biocomposites (a) and (b) (1000 \times) with scale bar of 45 μm .

This indicates that the PALF bundle structure was broken during processing. Most likely, the interfibril cementing force was overcome by shear forces during extrusion. The obvious benefit of this is reflected in the improved fiber dispersion in matrix and the improved fiber reinforcement efficiency thanks to the increase in aspect ratio of the fiber.

3.8. Water absorption

The results of the water absorption experiments for the soy based bioplastic and PALF reinforced soy based biocomposites are shown in Fig. 13. It is well known that a major problem of soy protein plastic is the higher water absorption, which can be reached about 363% at room temperature for same period of time [2]. The water

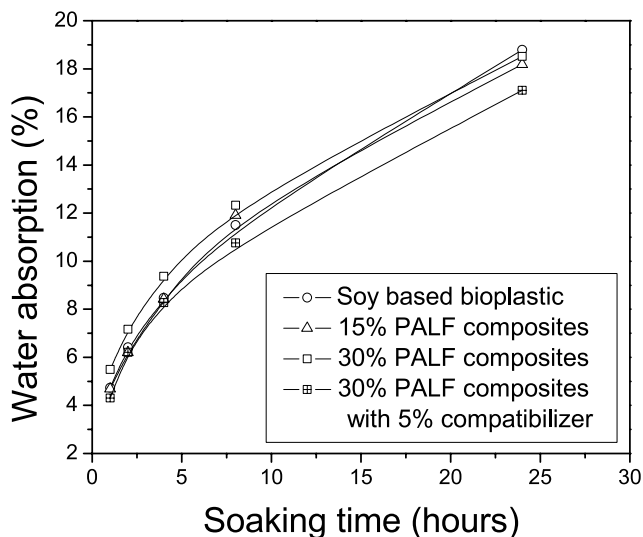


Fig. 13. Water absorption of soy based bioplastic and PALF reinforced soy based biocomposites.

absorption of the soy based bioplastic was 18% following a 24 h soak. This indicates that blending is an effective way to increase water resistance of soy plastic. Soy based biocomposites have a similar water absorption behaviour to soy based bioplastics. Water absorption increased with soaking time, but the rate decreased at longer times. The 15 wt% PALF reinforced composites had water absorptions within error of the bioplastics, however, the 30% PALF reinforced soy based biocomposites had higher water absorption due to the water penetration into gaps between the fiber and matrix. When 5% compatibilizer was used to increase the interaction between fiber and matrix in 30% PALF based biocomposites, the water absorption decreased, which is consistent with increased interaction between the fiber and matrix for these specimens.

4. Conclusion

The green composites from PALF and soy based thermoplastic have been fabricated by extrusion and injection molding. Mechanical properties including impact strength, tensile and flexural properties of 30 wt% PALF reinforced composites were significantly improved, compared with those of soy based biothermoplastic. In addition, the mechanical properties also improved adding PEA-g-GMA as a compatibilizer. The dispersion of PALF fiber in soy based bioplastic matrix reduced with increases in fiber content, but improved upon adding the compatibilizer. FTIR spectra show evidence of interactions between PALF and PEA-g-GMA due to the diminishing epoxy peak at 908 cm^{-1} . This is due to the reaction between hydroxyl group in PALF and epoxy group in PEA-g-GMA. In addition, water absorption of compatibilized composites reduced compared with uncompatibilized one. The above

factors indicate that the interfacial adhesion between fiber and matrix improved after adding PEA-g-GMA so that stresses can be transferred easily from matrix to fiber and hence the mechanical properties of the composites improved. The diameter of PALF in bundle state was 100 μm with fibril diameter of 4 μm . After adding to the soy based bioplastic, bundle structure of PALF was broken so that most of fiber became fibril. This is due to the weak cementing force between fibril, which can be overcome during processing and resulted in good separation of fiber in matrix.

Acknowledgements

The financial support from USDA-NRI (Grant No. 2001-35504-10734) and GREEN (Generating Research and Extension to meet Economic and Environmental Needs) (No. GR02-066) are gratefully acknowledged for this research. Authors also thanks to ADM (Decatur, IL), and Bayer Corp. (Pittsburgh, PA) for their supplying soy flour and polyester amide, respectively.

References

- [1] Catsimpooolas N, Kenney JA, Meyer EW, Szuhaj BF. *J Sci Food Agri* 1971;22(9):448–50.
- [2] Mo X, Sun X. *J Am Oil Chem Soc* 2002;79(2):197–202.
- [3] Wang S, Sue HJ, Jane J. *J Macromol Sci Pure Appl Chem* 1996; A33(5):557–69.
- [4] Zhang J, Mungara P, Jane J. *Polymer* 2001;42(6):2569–78.
- [5] Mo X, Sun XS, Wang Y. *J Appl Polym Sci* 1999;73(13):2595–602.
- [6] Liang F, Wang Y, Sun XS. *J Polym Eng* 1999;19(6):383–93.
- [7] Paetau I, Chen C-Z, Jane J. *Ind Eng Chem Res* 1994;33(7):1821–7.
- [8] Mungara P, Chang T, Zhu J, Jane J. *J Polym Environ* 2002;10(1/2): 31–7.
- [9] John J, Bhattacharya M. *Polym Int* 1999;48(11):1165–72.
- [10] Drzal LT, Mohanty AK, Tummala P, Misra M. *Polym Mater Sci Eng* 2002;87:117–8.
- [11] Mohanty AK, Misra M, Hinrichsen G. *Macromol Mater Eng* 2000; 276/277:1–24.
- [12] Mohanty AK, Misra M, Drzal LT. *J Polym Environ* 2002;10(1/2): 19–26.
- [13] Tummala P, Mohanty AK, Misra M, Drzal LT. Eco-composite materials from novel soy protein-based bioplastics and natural fibers. The 14th international conference on composite materials (ICCM-14), San Diego, CA, USA. July 14–18; 2003.
- [14] Lodha P, Netravali AN. *J Mater Sci* 2002;37(17):3657–65.
- [15] Liu W, Mohanty AK, Askeland P, Drzal LT, Misra M. *Polymer* 2004; 45(22):7589–96.
- [16] Mukherjee PS, Satyanarayana KG. *J Mater Sci* 1986;21:51–6.
- [17] Mishra S, Mohanty AK, Drzal LT, Misra M, Parija S, Nayak SK, Tripathy SS. *Compos Sci Technol* 2003;63(10):1377–85.
- [18] Mishra S, Tripathy SS, Misra M, Mohanty AK, Nayak SK. *J Reinf Plast Compos* 2002;21(1):55–70.
- [19] Luo S, Netravali AN. *Polym Compos* 1999;20(3):367–78.
- [20] Devi LU, Bhagawan SS, Thomas S. *J Appl Polym Sci* 1997;64(9): 1739–48.
- [21] Bhattacharyya TB, Biswas AK, Chatterjee J, Pramanick D. *Plast Rubber Compos Process Appl* 1986;6(2):119–25.
- [22] Liu W, Mohanty AK, Misra M, Askland P, Drzal LT, Fabrication and properties of green composites from soy based plastic and natural fiber, Polymer Processing Society Annual Meeting and 20th Anniversary, June 20–24, 2004, Akron, Ohio. PPS-20 Conference Proceedings, Paper Number: 135.
- [23] Nielsen LE, Landel RF. *Text Res J* 1994;64(11):696.
- [24] Fu SY, Lauke B. *Compos Sci Technol* 1998;58(3/4):389–400.
- [25] Peijs T, Garkhail S, Heijnenrath R, Van Den Oever M, Bos H. *Macromol Symp* 1998;127:193–203.
- [26] Crosby JM, Drye TR. *Mod Plast* 1986;63(11):74–84.
- [27] Kim HC. *Soc Automot Eng* 1998;SP-1340:167–71.
- [28] Tsai C-H, Chang F-C. *J Appl Polym Sci* 1996;61(2):321–32.